Catalysis Letters Vol. 109, Nos. 3–4, July 2006 (© 2006)
DOI: 10.1007/s10562-006-0070-6

Performance of Pt/MgAPO-11 catalysts in the hydroisomerization of *n*-dodecane

Xiaomei Yang,[a,b] Zhusheng Xu,[a] Zhijian Tian,[a,*] Huaijun Ma,[a,b] Yunpeng Xu,[a] Wei Qu,[a] and Liwu Lin[a,c]

[a]*Laboratory of Natural Gas Utilization and Applied Catalysis, Dalian Institute of Chemical Physics, Chinese Academy of Sciences, 457 Zhongshang Road, Dalian 116023, P.R. China*
[b]*Graduate School of the Chinese Academy of Sciences, 19 Yuquan Road, Beijing 100049, P.R. China*
[c]*State Key Laboratory of Catalysis, Dalian Institute of Chemical Physics, Chinese Academy of Sciences, 457 Zhongshang Road, Dalian 116023, P.R. China*

Received 9 January 2006; accepted 20 March 2006

MgAPO-11 molecular sieves with varying Mg contents synthesized by the hydrothermal method were used as supports for bifunctional Pt/MgAPO-11 catalysts. MgAPO-11 molecular sieves and the corresponding catalysts were characterized by X-ray diffraction (XRD), X-ray fluorescence spectroscopy (XRF), temperature-programmed desorption of NH_3 (NH_3-TPD), differential thermogravimetric (DTG) analysis, temperature-programmed reduction of H_2 (H_2-TPR), H_2 chemisorption and catalytic reaction evaluation. The results indicated that the acidity generated *via* the substitution of Mg^{2+} for Al^{3+} in the framework increased with the Mg content. Acting as acidic components, the MgAPO-11 molecular sieves loaded with Pt were tested in the hydroisomerization of *n*-dodecane. Optimum isomer yield was obtained over the Pt/MgAPO-11 catalyst that had neither the highest acidity nor the highest Pt loading among the tested catalysts. In fact, the activity and the isomer yield both could attain a maximum on 0.5 wt.% Pt/MgAPO-11 catalysts with differing Mg contents. A lower Mg content resulted in an insufficient acidity, whilst a higher Mg content weakened the dehydrogenation/hydrogenation function of the Pt. These inappropriate balances between the acidic and the metallic functions of the catalysts would lead to low activities and isomer yields. On the other hand, the 0.5 wt.% Pt/MgAPO-11(3) catalyst was found to have a good balance between the acidic and the metallic functions, and thus exhibited both high activity and isomer yield in comparison with the conventional 0.5 wt.% Pt/SAPO-11 catalyst.

KEY WORDS: hydroisomerization; *n*-dodecane; MgAPO-11; AEL molecular sieves.

1. Introduction

Hydroisomerization of *n*-alkanes to branched alkanes is one of the main routes to produce high octane number gasoline blending components, to enhance low temperature performance of diesels, and to obtain high viscosity index lube oils [1–3]. Generally, isomerization reactions are carried out over bifunctional catalysts containing metallic sites for dehydrogenation/hydrogenation, and acidic sites for skeletal isomerization *via* carbenium ions [4–6]. In recent years, bifunctional catalysts based on SAPO-11 have been developed for the hydroisomerization of *n*-alkanes [7–15]. The catalysts exhibit excellent catalytic properties due to the special pore structure (one-dimensional channel system with 10-membered ring openings of 0.39 nm × 0.63 nm pore diameter) and the moderate acidity of the SAPO-11 support. It is known that the Brønsted acid sites that are indispensable for the bifunctional isomerization catalysts are generated by the substitution of the P^{5+} ions by the Su^{4+} ions in the framework of the AlPO-11 with an AEL topology. Other elements, such as the Me^{2+} ions, can also be substituted into the AlPO-11 framework and generate the Brønsted acid sites. These substituted materials can then be used in the acid-catalyzed conversion of *n*-alkanes [16–19]. Hartmann and Elangovan have studied the influence of the pore diameter of magnesium-containing molecular sieves on the product selectivity of *n*-decane conversion. They found that over a large-pore catalyst of Pt/MgAPO-5, hydrocracking was predominant, whereas isomerization was dominating over medium-pore Pt/MgAPO-11 and Pt/MgAPO-41 catalysts [18]. However, to our knowledge, besides the pore size, other chemical properties, such as the acidity as well as the balance between the acidic sites and the metallic sites, are also important for the enhancement of the catalytic performance of isomerization. In order to optimize the reaction performance of the Pt/MgAPO-11 catalyst that is comparable to the conventional Pt/SAPO-11 catalyst for the hydroisomerization of long-chain *n*-alkanes, we have studied the special contribution of the acidity (the amount and strength of the acid sites) and the metallic properties of the Pt/MgAPO-11 catalyst to the activity and the isomer yield of *n*-dodecane hydroisomerization. The stability of Pt/MgAPO-11 catalyst was also investigated.

*To whom correspondence should be addressed.
E-mail: tianz@dicp.ac.cn

2. Experimental

2.1. Catalyst preparation

For the synthesis of molecular sieves with an AEL structure, phosphoric acid (85 wt.% H_3PO_4), pseudoboehmite (78.6 wt.% Al_2O_3), silica sol (30 wt.% SiO_2) and magnesium nitrate hexahydrate were used as the sources for phosphorus, aluminum, silicon and magnesium, respectively, and di-*n*-propylamine was used as the template. In the synthesis process, the raw materials were put together according to a preset order, and then stirred until homogenous gels were obtained. The gels were sealed in stainless-steel autoclaves lined with polytetrafluorethylene (PTFE) and crystallized at 200 °C for 48 h. The solid products recovered by centrifugation were washed with deionized water, dried overnight at 110 °C, and then calcined at 560 °C for 24 h in air. The gel compositions in molar ratio for these molecular sieves were given in table 1.

The powder of the calcined molecular sieves were pressed, crushed and sieved to obtain particles with 20–40 mesh. Catalysts loaded with Pt were obtained by an incipient wetness impregnation method with an aqueous H_2PtCl_6 solution at room temperature. Four catalysts with Pt load of 0.1, 0.25, 0.50 and 0.75 wt.% were prepared. After impregnation overnight, the catalysts were dried at 120 °C for 4 h, and finally calcined at 480 °C for 4 h.

2.2. Characterization

X-ray powder diffraction (XRD) patterns were recorded on a PANalytical X'Pert PRO diffractometer fitted with Cu $K\alpha$ radiation (λ = 1.5404 Å). Chemical composition analyses were determined with a Philips Magix X-ray fluorescence spectrometer.

Acidities of the samples were characterized by temperature-programmed desorption of ammonia. Before the adsorption of NH_3, the sample (0.1 g) was pretreated at 350 °C in helium (40 ml/min) for 30 min. Then the sample was cooled down to 100 °C and ammonia was injected into the helium stream until saturation was reached. The desorption process was monitored with a thermal conductivity detector at a temperature ramp from 100 to 600 °C, with a heating rate of 20 °C/min.

Differential thermogravimetric (DTG) analysis was carried out under an air atmosphere, using a Perkin–Elmer TGA 7 in the temperature range of 50–600 °C. The sample weight was 10 mg, and the heating rate was 10 °C/min, with an air flow rate of 20 ml/min.

H_2-TPR experiments were carried out with a home-made apparatus. All samples (0.1 g) were first pretreated at 350 °C in Ar (40 ml/min) for 30 min, and then cooled to room temperature. For TPR measurements, the samples were heated from ambient temperature to 620 °C at a rate of 20 °C/min in a 5 vol.% H_2/Ar (40 ml/min) flow and held at 620 °C for 20 min.

Pulse H_2 chemisorption experiments were also performed with the same apparatus as in the TPR measurements to determine the Pt dispersion of the catalysts. Prior to H_2 chemisorption, the catalysts were prereduced *in situ* with H_2 at 450 °C for 2 h. Then the samples were flushed with Ar for 1.5 h at 500 °C, and finally cooled down to ambient temperature in an Ar stream, where they were held for 0.5 h. H_2 chemisorption was measured at room temperature. The H_2 gas was injected till the adsorption had reached saturation. The volume of adsorbed H_2 was measured and used to calculate the Pt dispersion on the basis of the assumption that the stoichiometric ratio of H:Pt was 1:1.

Table 1
Gel compositions in molar ratio for the synthesis of the molecular sieves

Sample	Al_2O_3	P_2O_5	SiO_2	MgO	T[a]	H_2O
SAPO-11	1.0	1.0	0.3	0	1.1	50
AlPO-11	1.0	1.0	0	0	1.1	50
MgAPO-11(0.5)	1.0	1.0	0	0.005	1.2	50
MgAPO-11(1)	1.0	1.0	0	0.01	1.2	50
MgAPO-11(3)	1.0	1.0	0	0.03	1.2	50
MgAPO-11(6)	1.0	1.0	0	0.06	1.2	50
MgAPO-11(9)	1.0	1.0	0	0.09	1.2	50

[a]T represents di-*n*-propylamine.

2.3. Catalytic reaction

Hydroisomerization of *n*-dodecane as a model reaction was carried out in a continuous flow fixed-bed stainless steel reactor with a H_2/*n*-C_{12} molar ratio of 15, and a weight hourly space velocity of 1 h^{-1}. The reaction was performed both at atmospheric pressure and at 8 MPa. For the reactions operated at atmospheric pressure, the amount of catalysts loaded was 0.75 g. Prior to the reaction, the catalysts were reduced *in situ* in a hydrogen stream at 400 °C for 4 h. Then, the temperature was decreased to the desired reaction temperature and the feed was introduced into the reactor through a micro-pump. The temperature was maintained at least for 1 h to establish a steady state before sampling. The products were analyzed using an on-line gas chromatograph (VARIAN CP-3800) fitted with flame ionization detector, and equipped with a capillary column (PONA) of 100 m in length. For the pressurized reactions, the catalyst load was 7.5 g. Before transferred to the reactor, the catalysts were reduced *ex situ* in a hydrogen stream at 400 °C for 4 h. Other operating procedures were the same as the atmospheric-pressure reactions. The products released from the valve linking to the condenser behind the reactor were collected in a flask and analyzed using the above-mentioned gas chromatograph.

3. Results and discussion

3.1. Acidity of MgAPO-11 molecular sieves

Chemical composition analyses of the as-synthesized MgAPO-11 molecular sieves in table 2 indicate that the Mg content in the solid samples increased as the ratio of MgO/Al_2O_3 in the incipient gels was increased. The XRD patterns (not shown here) of all the samples were identical to that of the AEL structure reported in the literature [20]. The unit cell volumes calculated according to the diffraction peaks were given in table 2. The results showed that the unit cell volume of the MgAPO-11 expanded as compared to that of AlPO-11, because the ionic radius of Mg^{2+} (0.66 Å) was larger than that of Al^{3+} (0.51 Å) [21]. Moreover, the unit cell volume increased with the increase of the Mg content, which indicated that more Mg was isomorphously substituted into the framework.

The profiles of NH_3-TPD (figure 1) of all molecular sieve samples showed a low temperature peak at about 225 °C, which was attributed to the ammonia desorbed from the weak acid sites [17,22,23]. Except for AlPO-11, a shoulder peak appeared at the high temperature range for the MgAPO-11 as well as the SAPO-11, which corresponded to the ammonia desorbed from the strong acid sites originating from the substitution of Mg^{2+} for Al^{3+} or Su^{4+} for P^{5+} (SAPO-11). The shoulder peak was centered at 400 °C for the MgAPO-11 and at 250 °C for the SAPO-11. This means that the strength of the acid sites generated by the substitution of Mg^{2+} for Al^{3+} was stronger than that generated by the substitution of Su^{4+} for P^{5+}. It has been proposed that the acid strength was correlated with the ionic radius [24] and the electronegativity [25] of the dopant, and with the $T\hat{O}_HT'$ angle of the protonated oxygen (O_H) with its nearest neighbor ions T and T′ in the framework [26]. MO calculations [27] and periodic *ab initio* quantum mechanical calculations [21] both revealed that the value of the OH stretching frequency, ν_{OH}, for Mg–O_H–P was lower than that of Al–O_H–Si. A lower value of ν_{OH} for Mg–O_H–P represents a weaker O–H bond, and thus a higher strength of the acid site. The results of NH_3-TPD also displayed that the high temperature peak became more apparent with the increase of the Mg content. This result suggested that the number of strong acid sites increased with the increase of the Mg content. The total number of acid sites calculated from the amount of ammonia desorbed was collected in table 2. It shows that for the MgAPO-11, with the increase of the Mg content, the total number of acid sites increased from 0.22 to 0.41 mmol/g, while AlPO-11 and SAPO-11 contained the lowest and the highest number of acid site, respectively.

Table 2
Some characteristics of the molecular sieves

Sample	Mg content (wt.%)[a]	Acidity (mmol/g)[b]	V (Å^3)[c]
SAPO-11	–	0.54	2075
AlPO-11	–	0.10	2057
MgAPO-11(0.5)	0.04	0.22	2076
MgAPO-11(1)	0.10	0.23	2075
MgAPO-11(3)	0.50	0.34	2080
MgAPO-11(6)	1.14	0.37	2089
MgAPO-11(9)	1.70	0.41	2107

[a]Denoted in the formula of MgO.
[b]Calculated on the basis of the amount of ammonia desorbed.
[c]Unit cell volume.

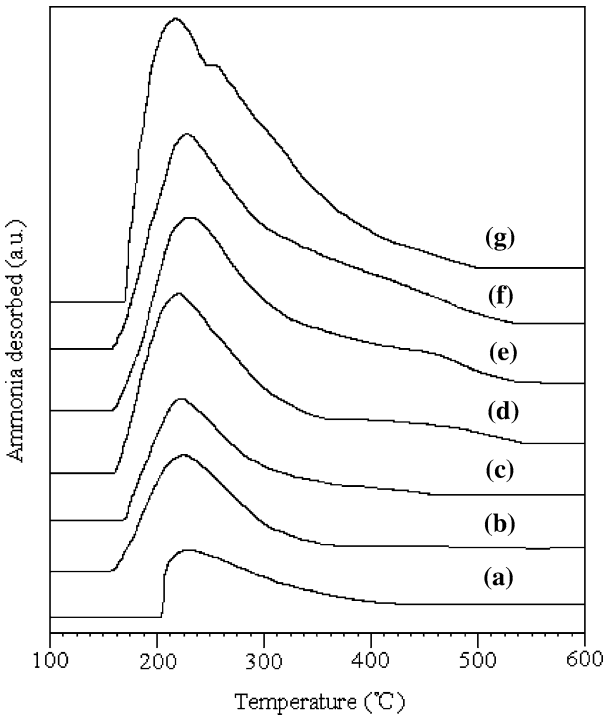

Figure 1. NH_3-TPD profiles of the calcined molecular sieves: (a) AlPO-11; (b) MgAPO-11(0.5); (c) MgAPO-11(1); (d) MgAPO-11(3); (e) MgAPO-11(6); (f) MgAPO-11(9); (g) SAPO-11.

The results of the DTG analyses are given in figure 2. The third peak of weight loss in region III was attributed to the decomposition of protonated templates that neutralized the negative charges of the framework, due to the substitution of Mg^{2+} for Al^{3+} or Su^{4+} for P^{5+} [28]. The peak in this region appeared only over the MgAPO-11 and SAPO-11. This fraction of the protonated amines was decomposed and transformed into Brønsted acid sites after calcination. The weight loss in region III became more intense as the Mg content was increased, and the peak maximum shifted to higher temperature with the increase of the Mg content. Both of these results indicated that the number and strength of Brønsted acid sites increased with the increase of the Mg content. The lower peak temperature of the SAPO-11 in region III also indicated that the acid strength of the SAPO-11 was lower than that of the MgAPO-11. These results were well consistent with those obtained by NH_3-TPD.

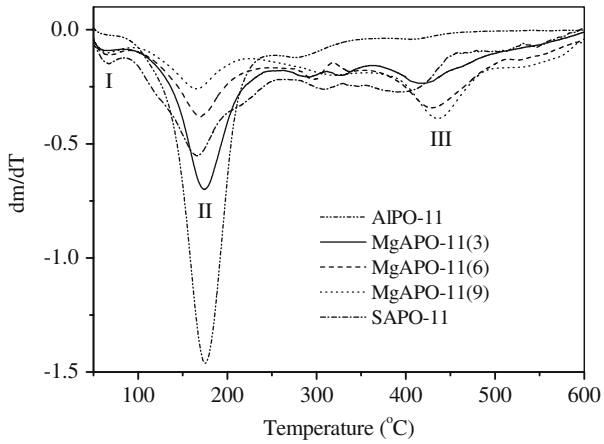

Figure 2. DTG curves of the as-synthesized AlPO-11, SAPO-11 and MgAPO-11 molecular sieves.

3.2. Interaction between Pt and the molecular sieves

Figure 3 showed the H_2-TPR profiles of supported 0.5 wt.% Pt catalysts. Two peaks were observed for all the catalysts. The first peak at the low temperature was assigned to the reduction of the platinum species that interacted weakly with the support. The second reduction peak at high temperature corresponded to the platinum species interacting strongly with the molecular sieves [29]. The second reduction peak for the Pt/AlPO-11 (curve a) appeared at 360 °C and for the Pt/SAPO-11 (curve b) shifted to 393 °C. This means that the interaction between the Pt species and the support for the Pt/SAPO-11 was stronger than that for the Pt/AlPO-11.

The TPR curves of the Pt/MgAPO-11s (curves c–e) were similar to that of the Pt/SAPO-11. The second reduction peak of Pt/MgAPO-11(3), Pt/MgAPO-11(6) and Pt/MgAPO-11(9) were centered at 403, 440 and 448 °C, respectively. The results indicated that the interaction between the Pt species and the MgAPO-11 became stronger with the increase of the Mg content.

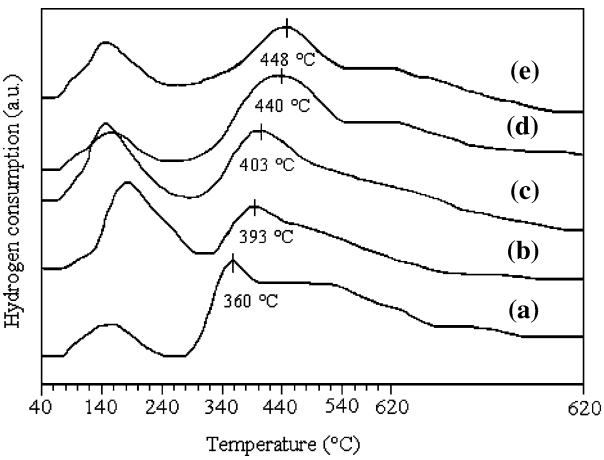

Figure 3. TPR results of supported 0.5 wt.% Pt catalysts: (a) Pt/AlPO-11; (b) Pt/SAPO-11; (c) Pt/MgAPO-11(3); (d) Pt/MgAPO-11(6); (e) Pt/MgAPO-11(9).

Furthermore, the interaction between the Pt species and the MgAPO-11 was stronger than that between the Pt species and the SAPO-11.

The results of H_2 chemisorption in table 3 demonstrated that the interaction between the Pt species and the MgAPO-11 could lead to a decrease in the Pt dispersion. Moreover, the stronger the interaction, the lower the dispersion of Pt. This suggests that there would be less Pt participating in the reaction with the increase of the Mg content.

3.3. Catalytic performance of Pt/MgAPO-11 in hydroisomerization of n-dodecane

3.3.1. Hydroisomerization of n-dodecane over Pt/MgAPO-11 catalysts with different Pt loadings

n-Dodecane conversions over Pt/MgAPO-11(3) catalysts with different Pt loadings were shown in figure 4. The mono-functional MgAPO-11(3) catalyst in the absence of Pt was almost inactive. When a small quantity of Pt (0.1 wt.%) was added, the conversion increased sharply. Then the conversion increased gradually with the increase of the Pt content until the Pt amount had reached 0.5 wt.%. Subsequently, the conversion remained almost unchanged with further increasing the Pt loading. The isomer yield changed with Pt content in the same trend as the conversion did. It is well known that during the hydroisomerization process of *n*-alkanes the noble metal catalyzes hydrogen transfer reactions (dehydrogenation/hydrogenation), while the isomerization and hydrocracking reactions occur on the acid sites [5]. In the absence of Pt, merely the moderate acidity of MgAPO-11(3) was not strong enough to catalyze *n*-dodecane conversion under the present reaction conditions. When a small amount of Pt was added, the transformation of *n*-dodecane could be initiated, but the whole reaction was dependent on the dehydrogenation/hydrogenation reactions catalyzed by the Pt sites. However, since the amount of Pt was so small, the Pt sites were not rich enough to allow the overall reaction to proceed smoothly. It was after the Pt content has exceeded a certain value that the catalyst could exhibit the best performance, and this was because the catalyst had established a proper balance between the acid and

Table 3
Results of H_2 chemisorption over supported 0.5 wt.% Pt catalysts

Catalyst	H_2 uptake ($ml/g_{cat.}$ STP)	H/Pt
Pt/SAPO-11	0.169	0.59
Pt/AlPO-11	0.130	0.45
Pt/MgAPO-11(0.5)	0.183	0.64
Pt/MgAPO-11(1)	0.177	0.62
Pt/MgAPO-11(3)	0.142	0.49
Pt/MgAPO-11(6)	0.108	0.38
Pt/MgAPO-11(9)	0.094	0.33

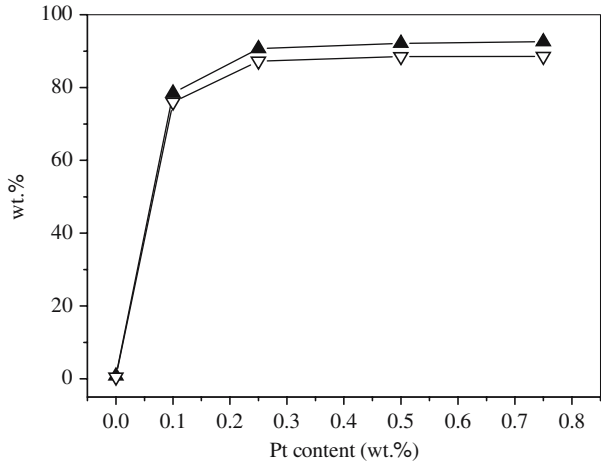

Figure 4. Conversion (-▲-) and isomer yield (-∇-) of *n*-dodecane hydroisomerization over Pt/MgAPO-11(3) catalysts as a function of the platinum content. Reaction conditions: $H_2/n\text{-}C_{12}$ (mol/mol) = 15; WHSV = 1.0 h^{-1}; P = atmospheric pressure; T = 280 °C.

the dehydrogenation/hydrogenation functions [14]. For the MgAPO-11(3) catalyst, it can be seen that 0.5 wt.% Pt was the optimum metal content for the hydroisomerization of *n*-dodecane.

3.3.2. Dependence of the catalytic performance on the Mg content

Figure 5 presents the conversion and the isomer yield of *n*-dodecane hydroisomerization over the 0.5 wt.% Pt/MgAPO-11 as a function of Mg content. When the Mg content was zero, the Pt/AlPO-11 catalyst was lack of strong acid sites needed to perform the acid cracking and skeleton isomerization of *n*-dodecane, and the main reaction was C–C bond breakage on the Pt sites [16]. So the activity (4%) and the isomer yield (1%) were both very low. As the Mg content was increased from zero to

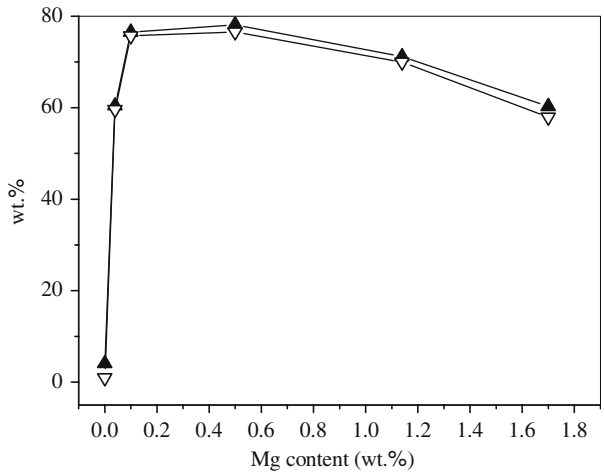

Figure 5. Conversion (-▲-) and isomer yield (-∇-) of *n*-dodecane hydroisomerization over 0.5 wt.% Pt/MgAPO-11 as a function of Mg content. Reaction conditions: $H_2/n\text{-}C_{12}$ (mol/mol) = 15; WHSV = 1.0 h^{-1}; P = atmospheric pressure; T = 260 °C.

0.04 wt.%, the activity and the isomer yield increased drastically. Then, the activity and the isomer yield increased gradually when the Mg content was increased from 0.04 to 0.50 wt.%. However, when the Mg content was further increased from 0.50 to 1.70 wt.%, the activity and the isomer yield were gradually reduced. These results revealed that the conversion and the isomer yield of *n*-dodecane hydroisomerization were not only dependent on the acidity of the MgAPO-11, due to the fact that the acidity of the catalyst was increasing linearly with the Mg content. Another important factor of the bifunctional catalyst, namely the properties of the metal component, should also be considered. For the 0.5 wt.% Pt/MgAPO-11 catalysts, when the Mg content was low, the acidity of the MgAPO-11 molecular sieve was too low to satisfy the need of the isomerization reaction, so the activity and the isomer yield were limited by the acidity, and would be increased with the increase of the acidity. When the Mg content was increased up to a certain value, the acidity of the MgAPO-11 molecular sieve was sufficient to carry out the isomerization reaction. Then, the activity and the isomer yield were both controlled by the dehydrogenation/hydrogenation function of the metal component. As mentioned above, when the Mg content was increased from 0.50 wt.% (Pt/MgAPO-11(3)) first to 1.14 wt.% (Pt/MgAPO-11(6)) and then to 1.70 wt.% (Pt/MgAPO-11(9)), the interaction between the Pt species and the MgAPO-11 became stronger and stronger. Moreover, this interaction was reducing the number of reactive metallic Pt sites. Therefore, though the acidity increased from MgAPO-11(3) to MgAPO-11(9), yet the interaction between the Pt and the MgAPO-11 had weakened the dehydrogenation/hydrogenation function of the metal, accordingly the activity and the isomer yield of the 0.5 wt.% Pt/MgAPO-11 decreased with a further increase of the acidity.

3.3.3. Hydroisomerization of n-dodecane over Pt/MgAPO-11(3) as a function of temperature

The dependence of the conversion of *n*-dodecane hydroisomerization on temperature, employing 0.5 wt.% Pt/MgAPO-11(3) as the catalyst, was displayed in figure 6. The conversion increased with the increase of the reaction temperature, whilst the isomer yield passed through a maximum with the increase of the conversion. These phenomena were similar to those over the conventional Pt/SAPO-11 catalyst and in complete agreement with the well-known reaction mechanism for the hydroisomerization of *n*-alkanes [2]. With the increase of the conversion, the branched isomers were consumed by hydrocracking, and maximum isomer yields of 89% and 81% over the Pt/MgAPO-11(3) and the Pt/SAPO-11 were obtained at 280 and 300 °C, respectively. From the results of NH_3-TPD it was known that the number of acidic sites on the

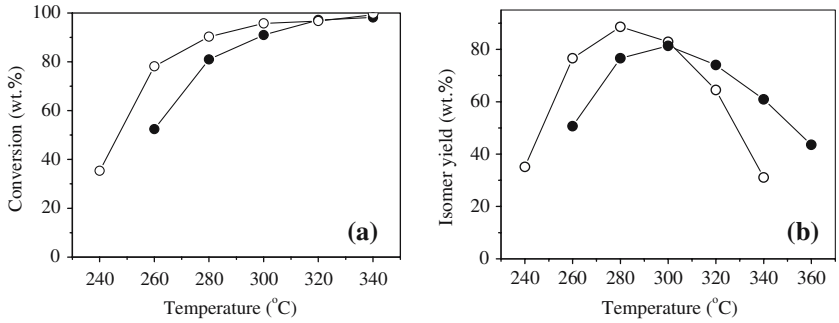

Figure 6. Conversion of *n*-dodecane (a) and isomer yield (b) on supported 0.5 wt.% Pt/SAPO-11 (-●-) and Pt/MgAPO-11(3) (-○-) catalysts. Reaction conditions: $H_2/n\text{-}C_{12}$ (mol/mol) = 15; WHSV = 1.0 h^{-1}; P = atmospheric pressure.

MgAPO-11(3) (0.34 mmol/g) was much less than that on the SAPO-11 (0.54 mmol/g). In addition, the dispersion of Pt (table 3) on the Pt/MgAPO-11(3) was also lower than that of the Pt/SAPO-11. So, the higher acid strength of the MgAPO-11(3), comparing with that of SAPO-11, was probably the reason for its higher activity and isomer yield.

3.3.4. *Catalytic performance of Pt/MgAPO-11(3) under elevated pressures*

Since the hydroisomerization processes of long-chain *n*-alkanes are often carried out at elevated pressures in industrial operation, we evaluated the catalytic performance of the 0.5 wt.% Pt/MgAPO-11(3) catalyst under an elevated pressure of 8 MPa, and the activity and selectivity are listed in table 4. As comparison, the data over the 0.5 wt.% Pt/SAPO-11 catalyst, which has generally been used in the industrial processes for the hydroisomerization of long-chain *n*-alkanes [7,13], are also included. It can be found that under an elevated pressure (8 MPa), the Pt/MgAPO-11(3) catalyst still exhibited excellent catalytic performance for the hydroisomerization of *n*-dodecane. A conversion of 87% and a selectivity of 84% could be achieved at 330 °C. Meanwhile, over a conventional Pt/SAPO-11 catalyst both the conversion and the selectivity were only 84% at 335 °C.

Table 4
Activity and selectivity (wt.%) of $n\text{-}C_{12}$ hydroisomerization over supported 0.5 wt.% Pt/MgAPO-11(3) and Pt/SAPO-11 catalysts[a]

Catalyst	T (°C)	Conversion	$S_{iso.}$	$Y_{iso.}$	$S_{cr.}$
Pt/MgAPO-11(3)	330	86.5	84.4	73.0	15.6
Pt/SAPO-11	335	83.9	84.3	70.7	15.7

[a]Reaction conditions: $H_2/n\text{-}C_{12}$ (mol/mol) = 15; WHSV = 1.0 h^{-1}; P = 8 MPa.

For industrial applications, besides high activity and selectivity, an excellent catalyst should possess an enduring stability for long-term operation. Therefore, the changes in activity and selectivity of the 0.5 wt.% Pt/MgAPO-11(3) catalyst at the initial stage was examined under both atmospheric and elevated (8 MPa) pressures, and the results are shown in figure 7. It can be seen that the activity, the isomerization selectivity and the yield maintained constant at both atmospheric and elevated pressures for 20 and 16 h of time on stream, respectively. These data indicated that the 0.5 wt.% Pt/MgAPO-11(3) catalyst were stable both in activity and selectivity at the initial stage of the catalytic operation. However, for the sake of practicability, the long-term life test should be performed in the pilot-plant, which will be reported in a future publication.

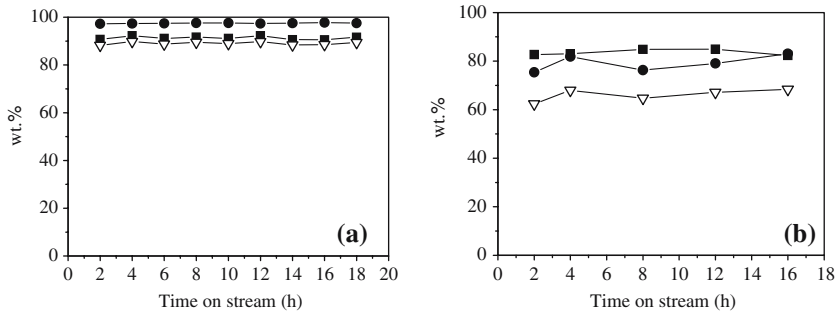

Figure 7. Hydroisomerization of *n*-dodecane as a function of time on stream over the supported 0.5 wt.% Pt/MgAPO-11(3) catalyst at atmospheric pressure (a) and at 8 MPa (b): (-■-) conversion; (-●-) selectivity; (-▽-) isomer yield. Reaction conditions: $H_2/n\text{-}C_{12}$ (mol/mol) = 15; WHSV = 1.0 h^{-1}; T = 270 °C (atmospheric pressure) and T = 335 °C (8 MPa).

4. Conclusions

The acidity of MgAPO-11 molecular sieves synthesized *via* hydrothermal method increased with the increase of the Mg content. In the hydroisomerization of long-chain *n*-alkanes, a proper balance between the acidic and the metallic functions was crucial for bifunctional Pt/MgAPO-11 catalysts. The activity and isomer yield of a 0.5 wt.% Pt/MgAPO-11 catalyst passed through a maximum with the increase of the Mg content. Lower Mg content resulted in an inadequately low acidity, whilst higher Mg contents weakened the dehydrogenation/hydrogenation function of Pt. Both of these inappropriate balances in bifunctionality resulted in low activity and isomer yield for the hydroisomerization of long-chain *n*-alkanes. The 0.5 wt.% Pt/MgAPO-11(3) catalyst, which was found to have a good balance between the acidic and the metallic functions, exhibited higher activity and isomer yield in comparison with the conventional 0.5 wt.% Pt/SAPO-11 catalyst.

References

[1] A. Chica and A. Corma, J. Catal. 187 (1999) 167.
[2] J. Weltkamp, Ind. Eng. Chem. Prod. Res. Dev. 21 (1982) 550.
[3] M.C. Claude and J.A. Martens, J. Catal. 190 (2000) 39.
[4] P.B. Weisz, Adv. Catal. 13 (1962) 137.
[5] H.L. Coonradt and W.E. Garwood, Ind. Eng. Chem. Process Des. Develop. 3 (1964) 38.
[6] M. Steijns, G. Froment, P. Jacobs, J. Uytterhoeven and J. Weitkamp, Ind. Eng. Chem. Prod. Res. Dev. 20 (1981) 654.
[7] S.J. Miller, US Patent 4 710 485 (1987).
[8] S.J. Miller, Micropor. Mater. 2 (1994) 439.
[9] B. Parlitz, E. Schreier, H.L. Zubowa, R. Eckelt, E. Lieske, G. Lischke and R. Fricke, J. Catal. 155 (1995) 1.
[10] J.M. Campelo, F. Lafont and J.M. Marinas, J. Catal. 156 (1995) 11.
[11] P. Mériaudeau, V.A. Tuan, V.T. Nghiem, S.Y. Lai, L.N. Hung and C. Naccache, J. Catal. 169 (1997) 55.
[12] J.M. Campelo, F. Lafont and J.M. Marinas, Appl. Catal. A 152 (1997) 53.
[13] J.M. Campelo, F. Lafont and J.M. Marinas, Appl. Catal. A 170 (1998) 139.
[14] M. Höchtl, A. Jentys and H. Vinek, Catal. Today 65 (2001) 171.
[15] J. Walendziewski and B. Pniak, Appl. Catal. A 250 (2003) 39.
[16] A. Vieira, M.A. Tovar, C. Pfaff, B. Méndez, C.M. López, F.J. Machado, J. Goldwasser and M.M. Ramírezde Agudelo, J. Catal. 177 (1998) 60.
[17] M. Höchtl, A. Jentys and H. Vinek, Micropor. Mesopor. Mater. 31 (1999) 271.
[18] M. Hartmann and S.P. Elangovan, Chem. Ing. Technol. 26 (2003) 12.
[19] S.P. Elangovan and M. Hartmann, J. Catal. 217 (2003) 388.
[20] PCPDFWIN, Version 1.30, 1997, JCPDS-ICDD, File 46-0647.
[21] F. Corà, C.R.A. Catlow, B. Civalleri and R. Orlando, J. Phys. Chem. B 107 (2003) 11866.
[22] S.B. Waghmode, S.K. Saha, Y. Kubota and Y. Sugi, J. Catal. 227 (2004) 425.
[23] G. Lischke, B. Parlitz, U. Lohse, E. Shreier and R. Fricke, Appl. Catal. A 166 (1998) 351.
[24] S. Hočevar, J. Batista and V. Kaučič, J. Catal. 139 (1993) 351.
[25] C. de las Pozas, R. Lopez-Cordero, J.A. Gonzalez-Morales, N. Travieso and R. Roque-Malherbe, J. Mol. Catal. 83 (1993) 145.
[26] H. Nur and H. Hamdan, Mater. Res. Bull. 36 (2001) 315.
[27] R. Carson, E.M. Cooke, J. Dwyer, A. Hinchliffe and P.J. O'Malley, Stud. Surf. Sci. Catal. 46 (1989) 39.
[28] R. Fernandez, M.V. Giotto, H.O. Pastore and D. Cardoso, Micropor. Mesopor. Mater. 53 (2002) 135.
[29] C.M. López, M.D. Sousa, Y. Campos, L. Hernández and L. García, Appl. Catal. A 258 (2004) 195.